Experimental Investigation and Mathematical Modeling of the Reaction between SO_2(g) and $CaCO_3$(s)-containing Micelles in Lube Oil for Large Two-Stroke Marine Diesel Engines

Lejre, Kasper H.L.; Glarborg, Peter; Christensen, Henrik; Mayer, Stefan; Kiil, Søren

Published in:
Chemical Engineering Journal

Link to article, DOI:
10.1016/j.cej.2020.124188

Publication date:
2020

Document Version
Peer reviewed version

Experimental Investigation and Mathematical Modeling of the Reaction between SO_2(g) and $CaCO_3$(s)-containing Micelles in Lube Oil for Large Two-Stroke Marine Diesel Engines

Kasper H. L. Lejre,[a] Peter Glarborg,[a] Henrik Christensen,[b] Stefan Mayer,[b] and Søren Kiil[,a]*

[a]Department of Chemical and Biochemical Engineering, Technical University of Denmark (DTU), Søltofts Plads 229, 2800 Kgs. Lyngby, Denmark

[b]MAN Energy Solutions, Teglholmsgade 41, 2450 Copenhagen SV, Denmark

* Corresponding author.

E-mail address: sk@kt.dtu.dk (S. Kiil)

Abstract

Sulfur dioxide, formed in combustion of sulfur-rich fuels in diesel engines, may oxidize and react with water to form corrosive H_2SO_4. However, the SO_2 may also be absorbed in the lube oil and consume $CaCO_3$-containing reverse micelles. In this study, the $CaCO_3$ + SO_2 reaction was investigated in a batch reactor setup at temperatures and pressures similar to those on the cylinder liner in an engine. The conversion of $CaCO_3$ and the formation of products were determined by Fourier Transform Infrared Spectroscopy (FTIR). $CaSO_3$ was the main product, but $CaSO_4$ was observed at extended residence times and increased temperature. The SO_2-$CaCO_3$ reaction exhibited only a small temperature dependence; the increase in the rate constant with temperature was partly

off-set because the absorption of SO_2 in the lube oil emulsion decreases at increased temperature. The reaction rate increased slightly with the initial water concentration due to increased SO_2 absorbance. A mathematical model for the batch reactor was set up and kinetic parameters were determined by fitting predictions to the experimental data. The model was then used to predict the $CaCO_3$ conversion in lube oil from SO_2 for conditions relevant to a full-scale engine application. Simulations showed that consumption of $CaCO_3$ from SO_2 is insignificant in a two-stroke marine diesel engine application and that the H_2SO_4-$CaCO_3$ reaction is far more important than the SO_2-$CaCO_3$ reaction.

1 Introduction

The so-called slow-steaming approach, where large vessels operate at a lower engine load, together with new engine designs and tunings, has led to increased sulfuric acid (H_2SO_4) condensation in the engines and strongly increased corrosive wear of the cylinder liner and piston rings [1–4]. To control corrosion, lubrication (lube) oils are formulated with base additives, commonly present as nanometer-sized $CaCO_3$ micelles [5–7]. At present, in some specific control areas, it is allowed to operate with a high sulfur content in the fuel if using an exhaust cleaning technology capable of reducing the emissions to a level equivalent to that of burning low-sulfur fuel [8,9]. It may therefore be cost-effective to burn high sulfur fuels; in the future perhaps even fuels with a sulfur content higher than today's limit of 3.5 wt.%, if concurrently installing an exhaust cleaning technology to comply with the local legislation. With fuel switching or new engine designs, the lube oil dosing has to conform to maintain its satisfactory performance.

A defective dosing of lube oil may have severe consequences, such as scuffing (direct metal to metal contact) [10,11]. It is therefore important to have general guidelines on how lube oil should be dosed onto the cylinder liners to limit corrosion at a minimal cost. To achieve this, an understanding of the formation of the relevant acids in the gas phase [10,12–14], the transport to the lube oil film [15–17], the neutralization mechanism by the base additives [17–35], and the corrosion of the liner material

[1,4,36–44] is pivotal. Information about how base additives ($CaCO_3$ micelles) are consumed is important because this facilitates determination of the lube oil flow rate to the cylinder liners and choice of base additive concentration. Research on sulfur neutralization has mainly focused on H_2SO_4, which is thought to be the main cause for the observed corrosive wear, and $CaCO_3$ consumption [4,37]. However, some studies indicate that also SO_2 can contribute to corrosive wear and $CaCO_3$ consumption [45–49]. Determination of the reaction kinetics of the $CaCO_3$-SO_2 reaction and assessment of its relative importance compared to the $CaCO_3$-H_2SO_4 reaction in terms of $CaCO_3$ reverse micelles consumption would be desirable. Nagaki and Korematsu [47,48] advocate that SO_2 absorbs into the lube oil film in an engine and forms H_2SO_4, which subsequently reacts with the cylinder liner and/or $CaCO_3$. Naegeli and Marbach [49] likewise found an increased wear rate for increasing SO_2 addition to the intake air through the formation of sulfurous acid (H_2SO_3). The formation of H_2SO_3 in lube oil may also contribute to consumption of $CaCO_3$. However, the addition of SO_2 to the intake air may have contributed to SO_3(g) formation upon the compression stroke, possibly increasing the condensation rate of H_2SO_4. The isolated effect of SO_2 on consumption of $CaCO_3$ in lube oil is therefore not clear.

It is known from other research fields that SO_2 reacts with $CaCO_3$. In wet flue gas desulfurization (FGD), SO_2 is removed (scrubbed) from flue gas by reacting with $CaCO_3$ in an aqueous slurry [50,51]. The mechanism is [50],

$$SO_2 + H_2O \rightarrow H^+ + HSO_3^- \quad (1)$$

$$HSO_3^- \rightarrow H^+ + SO_3^{2-} \quad (2)$$

$$2HSO_3^- + O_2 \rightarrow 2H^+ + 2SO_4^{2-} \quad (3)$$

$$Ca^{2+} + SO_4^{2-} + 2H_2O \rightarrow CaSO_4 \cdot 2H_2O(s) \quad (4)$$

The product of this reaction sequence is $CaSO_4$, same as for $CaCO_3$ reacting with H_2SO_4 [18,19]. However, if the system is not saturated with O_2, $CaSO_3$ is formed [50]:

$$Ca^{2+} + SO_3^{2-} + \frac{1}{2}H_2O \rightarrow CaSO_3 \cdot \frac{1}{2}H_2O(s) \quad (5)$$

The above illustrates that, besides $CaCO_3$ and SO_2, water and O_2 are required for the sulfation. The presence of water allows for absorption of SO_2 according to Eq. (1). The process is usually carried out in the temperature range 40-60 ºC, at a pH in the range 5-6, and at atmospheric pressure [50–52]. Also, the reaction between gaseous SO_2, in a humid simulated flue gas, and $CaCO_3$ particles has been investigated in a sand bed reactor [53]. Experiments showed that the oxygen content in the simulated flue gas (0-9%) had only a minor effect on the initial reaction rate, whereas the relative humidity (0.24-0.92) and particle diameter (4-100 μm) had significant effects [53]. The temperature dependency of the reaction was small in the investigated range (40-80 ºC). The reaction between gaseous SO_2 and $CaCO_3$ particles forms both $CaSO_3$ and $CaSO_4$ at 23 ºC and the reaction is significantly enhanced in the presence of water vapor [54,55]. The reaction conditions of the wet and dry desulfurization processes are different to those prevailing in a lube oil film, primarily due to the presence of the lube oil phase itself. However, the conditions in an engine, with SO_2 and O_2 in the combustion chamber, water condensing on the liner, absorption of SO_2 in the oil, and presence of reactive $CaCO_3$ reverse micelles [12,15,16,19,56], appear favorable for reaction in the lube oil film.

The scope of the present work is to investigate the reaction between gaseous SO_2 and $CaCO_3$ reverse micelles in lube oil in the presence of water and O_2 and to assess the consumption of $CaCO_3$ in the lube oil by SO_2. The reactants are pressurized in a batch reactor at specific conditions such as residence time, Ca/S molar ratio, pressure, temperature, and water content. Upon an experiment, the lube oil is analyzed and the conversion of $CaCO_3$ and the products are determined. Reaction kinetics are derived by setting up a model for the batch reactor and fitting modeling predictions to the experimental data. The mathematical model is then used to investigate the importance of the SO_2-$CaCO_3$ reaction at marine diesel engine conditions.

2 Experimental section

2.1 Materials

Lube oil from Infineum, with a base number (BN) value of 100±2, which corresponds to 8.9±0.18 wt.% $CaCO_3$, was used. The BN is a measure of the alkaline concentration present in a lube oil, expressed in terms of milligrams KOH in a 1 g lube oil sample [57]. The two gas mixtures (technical air and 1 mol% SO_2 in air) were obtained from AGA A/S. For the Karl Fischer titration method, Hydranal Solvent-Oil, Hydranal Titrant 2, and Toluene were applied, all obtained from Sigma-Aldrich. The $CaSO_3 \cdot 0.5H_2O$ and $CaSO_4 \cdot 2H_2O$ powders were from Wako and Sigma-Aldrich, respectively, and the $CaCO_3$ powder was Faxe Bryozo limestone from Faxe, Denmark.

2.2 Batch reactor setup

The reaction was investigated in a stirred batch reactor (Parr 4575) at temperatures and pressures similar to those of the cylinder liner in a full-scale marine diesel engine. The batch reactor setup is illustrated in Figure 1.

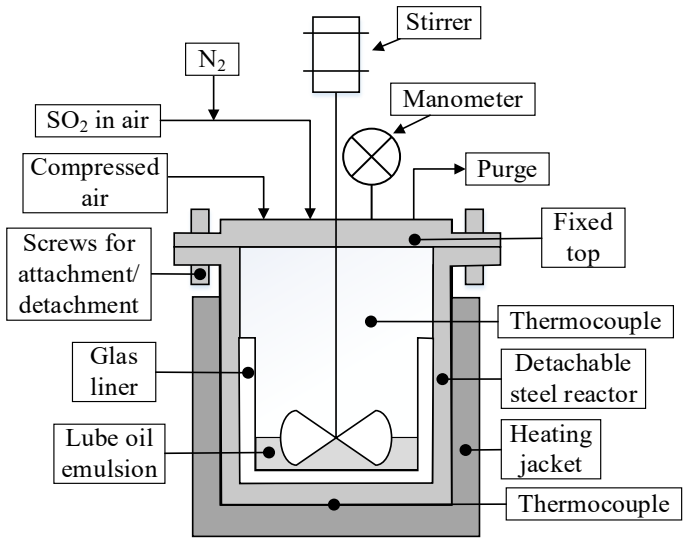

Figure 1. Illustration of the high-pressure and high-temperature batch reactor setup.

Lube oil and water were weighed in a glass beaker (liner) prior to an experiment to determine the water and $CaCO_3$ contents in the emulsion. Typical values were 9 g of lube oil and 0.5 g of demineralized water. The beaker was then placed inside the reactor. It was possible to achieve a

maximum pressure of around 200 bar and a maximum temperature of around 350 ºC in the reactor. The reactor was pressurized with technical air and/or with 1 mol% SO_2 in air. The lube oil was stirred during an experiment. The heating profile of the batch reactor is presented in Figure 2.

After the lube oil emulsion was placed inside the batch reactor, the latter was assembled, flushed three times with air, and a pressure leak test was carried out with air at 20 bar. The batch reactor was then gradually heated to a specific temperature and the heating was conducted under pressure (20 bar at room temperature) to keep as much of the added water in the liquid phase as possible. Temperature sensors were located inside the reactor and just below the bottom of the reactor; the difference between the two measurement points was generally below 10 ºC. The temperature used for data treatment was an average of the two measured values. When a specific temperature was reached, a mixture of 1 mol% SO_2 in air was introduced to the batch reactor till a specific pressure. After a specific residence time (τ), the gas phase was ventilated and the reactor was immediately flushed with N_2, while the reactor was cooled. During this flushing/cooling stage, the major part of the added water evaporated. The SO_2 was introduced after heating to a specific temperature to control the residence time and temperature. Using this procedure, all the water was kept inside the batch reactor during an experiment, limiting the evaporation of water from the lube oil.

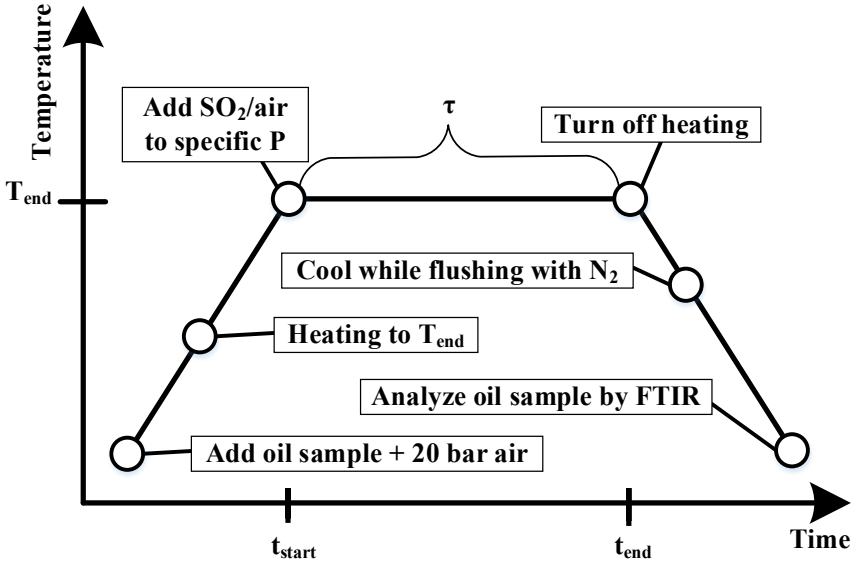

Figure 2. The temperature profile of the batch reactor setup during an experiment.

2.3 Analysis methods

The lube oil samples were analyzed by a Thermo Scientific Nicolet iS50 ATR-FTIR (Attenuated Total Reflectance Fourier Transform Infrared Spectroscopy) spectrometer. The use of FTIR allowed distinction between $CaCO_3$, $CaSO_3$, and $CaSO_4$. This is illustrated in Figure A1 in Supplementary Material (SM), where infrared spectra of the pure powder components are shown. In this way, the degree of reaction of $CaCO_3$ could be quantified and the reaction products could be determined [18]. The lube oil base number (BN) was calculated by a calibration curve relating the height of the $CaCO_3$ band from an infrared spectrum to the base number. The latter was determined by titration following a standard test method, ASTM D-2896 [57]. The procedure is described by Lejre et al. [18]. Applying this method made it possible to determine the degree of conversion of $CaCO_3$ after reaction with SO_2. The water content in the fresh lube oil was measured by Karl Fischer titration using a 701 KF Titrino autotitrator from Metrohm. Toluene was used to assist the Hydranal-Solvent Oil in dissolving the lube oil sample sufficiently. The water content in the fresh 100 BN lube oil was determined to 1.1 wt.% with a sample standard deviation of 0.3 wt.%, based on four measurements. The overall water

content includes the water already present in the lube oil (taken as the averaged value, 1.1 wt.%) as well as the added demineralized water.

Blank experiments were conducted according to the experimental procedure described, but without SO_2 in the gas phase. The results revealed that all the added demineralized water evaporated during the cooling stage and that no effect of the experimental procedure on the resulting lube oil infrared spectra was found. Consequently, the observed change in the $CaCO_3$ band, when SO_2 is present in the gas phase, is the isolated effect of reaction with SO_2. The calibration curves determined earlier [18] are therefore useful in quantifying the $CaCO_3$ in a lube oil sample for the SO_2 experiments. The resulting infrared spectra together with an unused 100 BN lube oil spectrum are shown in Figure A2 in Supplementary Material.

To get an idea of which products to expect, an infrared spectrum of a real drain oil sample was obtained (Figure A3 in SM). From titration results, the base number was around 20. Only $CaSO_4$ and $CaCO_3$ were detected in the drain oil sample; the $CaSO_3$ band at 800-1000 cm^{-1} was absent in the spectrum. Even though no observations of $CaSO_3$ in an engine application have been reported in literature, $CaSO_3$ could still be intermediate in formation of $CaSO_4$.

3 Results and discussion

3.1 Batch reactor experiments

The aim of the batch reactor experiments is to clarify whether SO_2 and $CaCO_3$ reverse micelles react in a lube oil emulsion and, if so, determine a reaction rate and identify which products are formed. The reaction is investigated at conditions relevant for the cylinder liner in a full-scale two-stroke engine, varying the temperature, residence time, and initial water concentration.

3.1.1 Product determination and effect of temperature

An experiment at room temperature was carried out with a Ca/S ratio of around unity and a total pressure in the batch reactor of 50 bar of 1 mol% SO_2 in air. The Ca/S molar ratio is defined as the

initial molar ratio between $CaCO_3$ in the oil phase to SO_2 in the gas phase. 6.2 wt.% of water was initially present in the lube oil sample. The residence time was 60 minutes. Figure 3 compares the resulting infrared spectrum with those of a fresh 100 BN lube oil and the pure $CaSO_3$ spectrum, respectively.

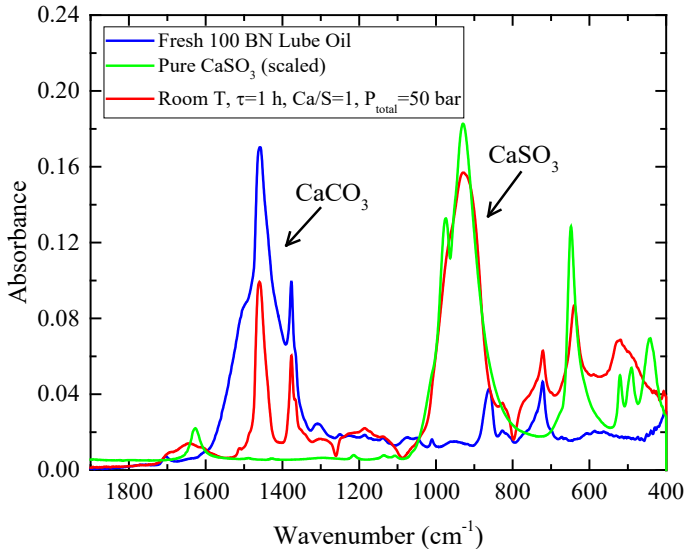

Figure 3. Infrared spectra from room temperature experiment (red), unused 100 BN lube oil (blue), and pure $CaSO_3$ (green). Experimental conditions: Ca/S=1, P_{total}=50 bar, 6.2 wt.% water in lube oil, and τ=60 min. Note, that a shift in baseline due to water is found in the range 400-1000 cm^{-1} and 1600-1700 cm^{-1} for the room temperature experiment spectrum (red).

By using calibration curve data for the $CaCO_3$ band [18], it was found that no $CaCO_3$ was left in the lube oil sample, thus the observed peak in the range around 1300-1500 cm^{-1} is some unknown component(s) present in the lube oil. The results in Figure 3 also show that no or very little $CaSO_4$ was formed, i.e., all $CaCO_3$ reacted to $CaSO_3$. Figure 4(a) shows spectra obtained as a function of temperature and in Figure 4(b), the resulting conversion of $CaCO_3$ together with the Ca/S molar ratios are shown. The conversion of $CaCO_3$ increases slightly with temperature (with exception of the 27 ^oC experiment). When the temperature is increased, the absorption of SO_2 to the lube oil emulsion decreases. Therefore, it is expected that the reaction rate constant will have a stronger temperature

dependence than depicted in Figure 4. The significantly higher conversion observed for the room temperature experiment (27 °C) is conceivably due to a larger absorption of SO_2 into the lube oil emulsion. In addition, SO_2 had an increased reaction time at lower temperatures, because the desorption time of SO_2 after an experiment may be increased at low temperature.

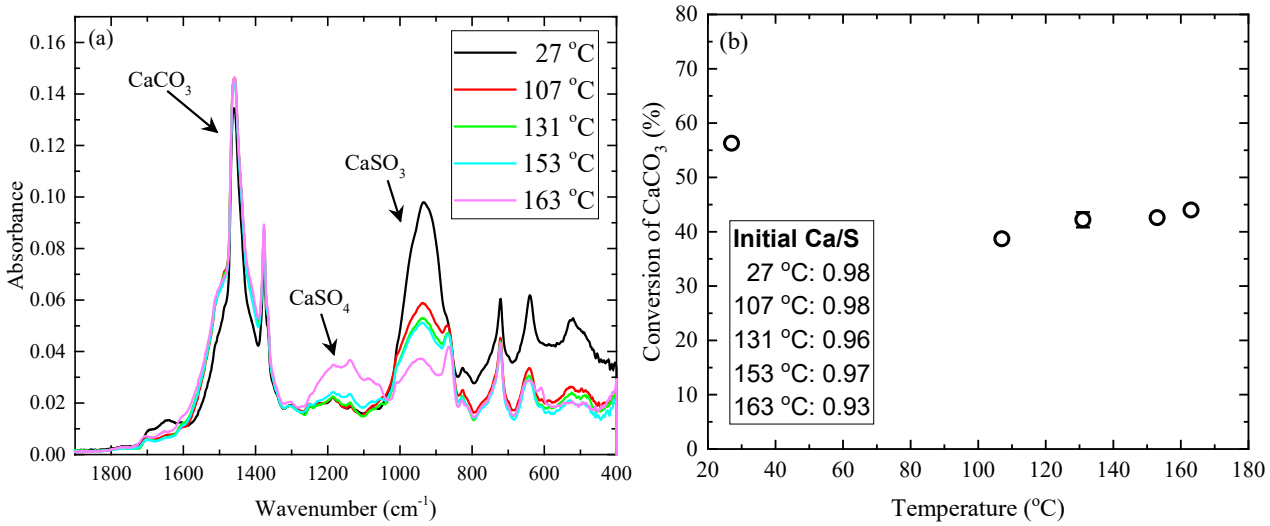

Figure 4. (a) Spectra of lube oil samples after being exposed to different temperatures for 10 minutes in the range 27-163 °C according to the procedure presented in Figure 2. Experimental conditions: P_{total}=90-105 bar, 6.6 wt.% overall initial water in lube oil, τ=10 min. (b) The effect of temperature on the conversion of $CaCO_3$ and the Ca/S molar ratio at the specific temperature. The error bars represent lower and upper conversions determined from two similar experiments and the data point is the averaged conversion. The theoretical maximum degree of $CaCO_3$ conversion is 100% because the Ca/S molar ratio is lower than one.

To investigate if the reaction between SO_2 and $CaCO_3$ is limited by chemical equilibrium, an experiment with a residence time of 24 hours was carried out with the following conditions: T=120 °C, Ca/S=0.90, P_{total}=90 bar, and 6.8 wt.% water in the lube oil emulsion. The resulting infrared spectrum revealed a complete consumption of $CaCO_3$, indicating that the conversion of $CaCO_3$ shown in Figure 4 was not limited by equilibrium in the system. According to the resulting spectrum (Fig.

A4 in SM), a small fraction of the $CaCO_3$ was converted to $CaSO_4$. However, no $CaSO_4$ was found for temperatures up to 153 ºC for a residence time of 10 minutes (Figure 4(a)). This implies that $CaSO_4$ is formed from $CaSO_3$ in a secondary reaction or through a change in mechanism. It was not possible to investigate the effect of temperature above 163 ºC with the present experimental configuration because the oil would ignite.

3.1.2 Effect of residence time

Figure 5 shows the effect of residence time on the reaction of $CaCO_3$ with SO_2 at temperatures of 131 ºC and 153 ºC. Apparently, the reaction is fast initially and then slows down significantly with time. For the experiments carried out at 153 ºC, more $CaSO_4$ was observed at increased residence time, but the amount of $CaSO_3$ was more or less constant. This supports that $CaSO_3$ is formed initially followed by either oxidation of $CaSO_3$ to $CaSO_4$ or formation of $CaSO_4$ directly from the SO_2-$CaCO_3$ reaction.

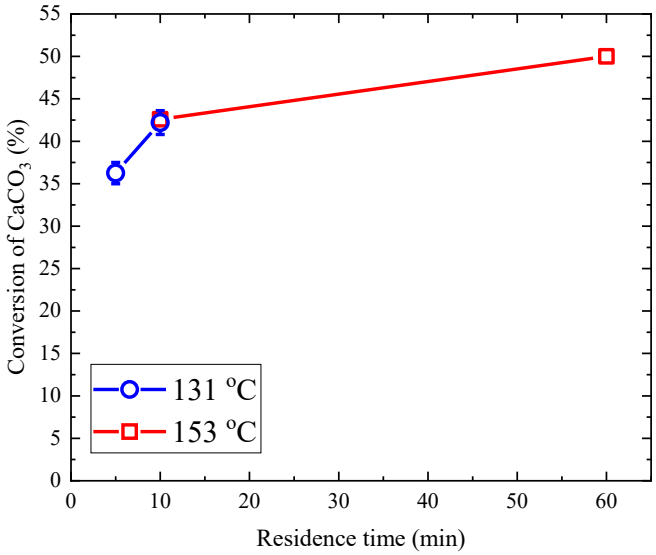

Figure 5. The effect of varying the residence time on the degree of conversion of $CaCO_3$ at temperatures of 131 and 153 ºC. Experimental conditions. P_{total}=90-105 bar, 6.6 wt.% water in the lube oil emulsion, and Ca/S around one. The error bars represent lower and upper conversions determined from two experiments and the data points are the averaged conversions. The spectra can be found in Figure A5 in Supplementary Material.

3.1.3 Effect of water concentration

The effect of initial water concentration (1.1-12%) in the lube oil emulsion on the $CaCO_3$ conversion at 131 °C is shown in Figure 6. The conversion of $CaCO_3$ increases linearly with the initial water content in the lube oil. Conceivably, this can be attributed mostly to an increased SO_2 absorption in the lube oil emulsion because the solubility of SO_2 is higher in water than in the base stock of the lube oil [56,58], i.e., increasing the SO_2 concentration in the lube oil emulsion. However, the reaction may also depend on the water concentration. An experiment at room temperature, without any added water to the lube oil but otherwise conditions similar to those of Figure 3, showed a significantly reduced conversion of $CaCO_3$ of only 25.6%. The initial molar ratio between water and $CaCO_3$ was calculated to 0.7, meaning that sufficient water was present assuming that $CaSO_3 \cdot ½H_2O$ is formed from the reaction. However, possibly some of the water was not available for the reaction; the Karl Fischer titration gives only the total amount of water in a sample. Nevertheless, the effect of water content on the conversion of $CaCO_3$ is significant and apparently the reaction between SO_2 and $CaCO_3$ proceeds only when water is present.

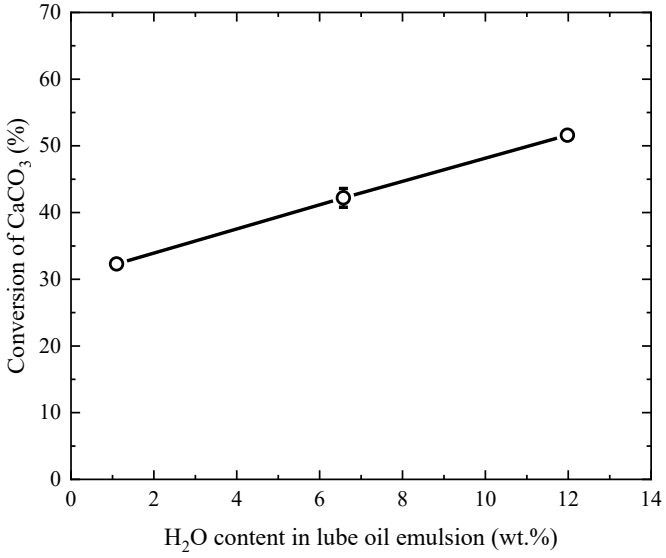

Figure 6. The effect of varying the initial water content in the lube oil emulsion on the degree of conversion of $CaCO_3$. Experimental conditions: P_{total}=90 bar, T=131 °C, τ=10 min, and Ca/S around

1. The error bars represent lower and upper conversions determined from two experiments and the data point is the averaged conversion.

3.1.4 Stability of $CaSO_3$

The present results show that the main product formed between SO_2 and $CaCO_3$ is $CaSO_3$. However, at increased temperature (Figure 4(a)) and residence time (Figures A4 and A5 in SM) also $CaSO_4$ was formed. This indicates that $CaSO_3$ can be oxidized to $CaSO_4$ at elevated pressure and temperature. However, heating a $CaSO_3$ containing lube oil sample in an oven at atmospheric pressure at 150 ^oC did not lead to the formation of $CaSO_4$, showing that $CaSO_3$ is stable over time. There were indications of $CaSO_4$ formation under pressurized conditions (80 bar, at 150 ^oC for one hour), but results were not conclusive, since the loss of water from the sample resulted in a shift in baseline (Figures A6 and A7 in SM). Overall, the observations indicate that $CaSO_3$ is stable once formed. Apparently, $CaCO_3$ starts to be converted into $CaSO_4$ by reaction with SO_2 when the concentration of $CaSO_3$ reaches a certain level; at this stage, the formation rate of $CaSO_3$ is significantly reduced (or even stopped).

3.1.5 Neutralization ability of $CaSO_3$

The neutralization ability of $CaSO_3$ was investigated by converting all initial $CaCO_3$ to $CaSO_3$ followed by addition of H_2SO_4 (96 wt.%). A lube oil emulsion with 6.2 wt.% water was pressurized to 50 bar of 1 mol% SO_2 in air at room temperature. An FTIR spectrum recorded after one hour of residence time confirmed that all $CaCO_3$ had converted to $CaSO_3$. Then, H_2SO_4 was added to the lube oil sample, making sure that $CaSO_3$ was in molar excess compared to H_2SO_4. The presence of $CaSO_3$ in the lube oil prevented accurate determination of the BN by the titration method, but the resulting infrared spectra (Figure A8 in SM) revealed that the $CaSO_3$ was converted to $CaSO_4$, possibly through the reaction:

$$CaSO_3 + H_2SO_4 \rightarrow CaSO_4 + SO_2 + H_2O \quad (6)$$

The release of SO_2 from the sample after addition of H_2SO_4 was verified by a gas detector. The occurrence of this reaction shows that the neutralization ability is retained when $CaCO_3$ reacts with SO_2 to form $CaSO_3$. Whether the $CaSO_3$-H_2SO_4 has a similar reaction rate as the $CaCO_3$-H_2SO_4 reaction is unknown.

3.2 Mathematical modeling of lube oil batch reactor

A mathematical model for the reaction in the batch reactor setup was developed. Model predictions were fitted to the experimental data to extract a kinetic expression for the $CaCO_3$-SO_2 reaction. This rate expression was then used in the model to investigate the relative importance of the $CaCO_3$-SO_2 and $CaCO_3$-H_2SO_4 reactions at engine conditions.

The assumptions underlying the batch reactor model were:

- The lube oil emulsion volume is well-mixed (no radial or axial concentration or temperature gradients).
- The only reaction in the lube oil is $CaCO_3$ (s) + SO_2 (aq) → $CaSO_3$ (s) + CO_2 (g) with a reaction rate of $(-r_A)$.
- SO_2 from the gas phase absorbs both in the lube oil and in the water. A combined expression for Henry's constant, H_L, dependent on the water concentration in the lube oil emulsion, is used.
- The effect of the water concentration on the conversion of $CaCO_3$ is reflected in the combined Henry's constant only.
- Even though SO_2 presumably only reacts with $CaCO_3$ in the presence of water, SO_2 present in the base stock of the lube oil is available for reaction, because water may be present in/near the $CaCO_3$ reverse micelles.
- The effect of O_2 can be disregarded because a large excess of O_2 compared to SO_2/$CaCO_3$ was present in the batch reactor experiments.

- Formation of $CaSO_3$ does not limit the $CaCO_3$-SO_2 reaction.
- The ideal gas law can be used to calculate the concentration of SO_2 in the gas phase.
- Only the transfer of SO_2 from the gas phase to the liquid phase has to be considered; release of SO_2 from the liquid phase to the gas phase can be disregarded.

3.2.1 Reaction rate expression

Since the reaction between SO_2 and $CaCO_3$ is assumed to form only $CaSO_3$, the simple overall reaction rate expression is given as:

$$(-r_A) = kC_{SO_2}^{L} C_{CaCO_3}^{L} \tag{7}$$

Here, $C_{SO_2}^{L}$ and $C_{CaCO_3}^{L}$ are the bulk concentrations of SO_2 and $CaCO_3$, respectively, in the lube oil emulsion, which consists of the lube oil and the added demineralized water. $C_{SO_2}^{L}$ is estimated from the absorption of gaseous SO_2 into the emulsion. The model takes into account the uptake of SO_2 from the gas phase to the lube oil emulsion followed by reaction between SO_2(aq) and $CaCO_3$(s). It includes mass balances for SO_2 in the gas phase and oil phase, respectively, and for $CaCO_3$ in the oil phase. An illustration of the system is shown in Figure 7. The reaction order of the water concentration in the lube oil emulsion is assumed to be zero. The effect of the water concentration on the reaction (Figure 6) is attributed to an increased SO_2 uptake from the gas phase and is reflected by the combined Henry's constant depending on the initial water concentration.

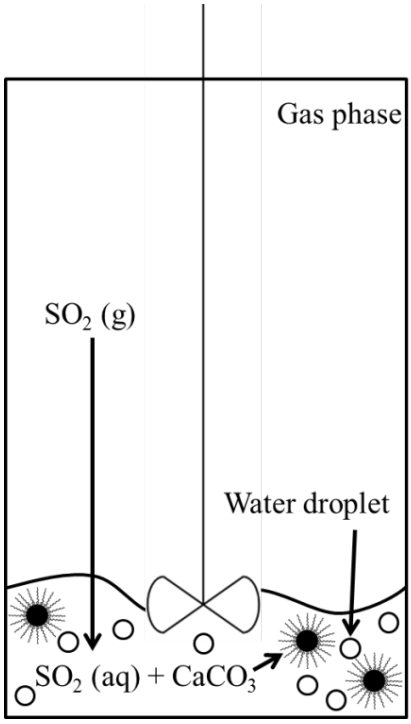

Figure 7. An illustration of the batch reactor setup: SO_2(g) has to be absorbed by the lube oil emulsion (oil and/or water) before it can react with the $CaCO_3$(s) in the lube oil.

3.2.2 Mass balance of SO_2 in the gas phase

The mass balance for the SO_2 in the gas phase is:

$$\frac{dC_{SO_2}^G}{dt} = -N_{SO_2}\frac{V_L}{V_G} \tag{8}$$

Here, N_{SO_2} (mol m^{-3} s^{-1}) is the absorption rate of SO_2 from the gas phase to the lube oil emulsion, calculated as [50]:

$$N_{SO_2} = K_G a\left(p_{SO_2}^G - p_{SO_2}^*\right) \tag{9}$$

K_G (mol m^{-2} bar^{-1} s^{-1}) is the overall mass transfer coefficient of SO_2 on gas basis, a (m^2 m^{-3}) is the specific gas-liquid interfacial area, $p_{SO_2}^G$ is the bulk partial pressure of SO_2 in the gas phase, and $p_{SO_2}^*$ is the partial pressure of gas-phase SO_2 in equilibrium with the bulk lube oil concentration $C_{SO_2}^L$. The

equilibrium relationship is given by Henry's law by introducing Henry's constant of the lube oil emulsion, H_L:

$$p^*_{SO_2} = H_L C^L_{SO_2} \tag{10}$$

The partial pressure of SO_2 in the gas phase, $p^G_{SO_2}$, is linked to the concentration of SO_2 in the gas phase by the ideal gas law:

$$p^G_{SO_2} = C^G_{SO_2} RT \tag{11}$$

The overall gas-side mass transfer coefficient, K_G, is given as [59]:

$$K_G = \frac{1}{\frac{1}{k_G} + \frac{H_L}{k_L}} \tag{12}$$

Here, k_G (mol m^{-2} s^{-1} bar^{-1}) is the gas film mass transfer coefficient and k_L (m s^{-1}) is the liquid film mass transfer coefficient.

3.2.3 Mass balance of SO_2 in the lube oil emulsion

In the lube oil emulsion, SO_2 enters from the gas phase and is consumed by the $CaCO_3$ reverse micelles. The mass balance of SO_2 in the lube oil emulsion is formulated as:

$$\frac{dC^L_{SO_2}}{dt} = N_{SO_2} - (-r_A) \tag{13}$$

$(-r_A)$ and N_{SO_2} are estimated from Eqs. (7) and (9), respectively.

3.2.4 Mass balance of $CaCO_3$ in the lube oil emulsion

$CaCO_3$ is consumed by reaction with SO_2,

$$\frac{dC^L_{CaCO_3}}{dt} = -(-r_A) \tag{14}$$

Three differential equations are thereby derived describing the concentration change over time in the batch reactor of SO_2 in the gas phase, Eq. (8), SO_2 in the lube oil emulsion, Eq. (13), and $CaCO_3$ in the lube oil emulsion, Eq. (14). The aim is to derive the reaction rate constant, k, given in Eq. (7), by fitting the model to the experimental data.

3.2.5 Initial conditions

Three initial conditions are needed: one for the $CaCO_3$ concentration in the lube oil, one for the SO_2 concentration in the gas phase, and one for the SO_2 concentration in the lube oil emulsion. The fresh lube oil was measured to have an average base number of 98.55 BN [18], which corresponds to a $CaCO_3$ concentration of 826 mol m^{-3} (835 mol m^{-3} in the water-free lube oil). The concentrations and reaction rates are based on the volume of the lube oil emulsion (lube oil + water), thus the water-free concentration of $CaCO_3$ is multiplied by the ratio of lube oil volume to lube oil emulsion. The initial concentration of SO_2 in the total gas phase is calculated by the ideal gas law using the partial pressure of SO_2 in the gas phase and the temperature. Lastly, it is assumed that the initial concentration of SO_2 in the lube oil emulsion is zero. The Ca/S molar ratio is defined as the initial molar ratio between $CaCO_3$ in the emulsion and SO_2 in the gas phase, calculated as:

$$\frac{Ca}{S} = \frac{C^L_{CaCO_3,0} V_L}{C^G_{SO_2,0} V_G} \tag{15}$$

If equal to e.g. 0.5, 50% conversion of the gaseous SO_2 is expected for complete conversion of the $CaCO_3$ reverse micelles in the lube oil emulsion.

3.2.6 Estimation of input parameters

The input parameters to the model include experimental conditions and estimated values of K_G, a, H_L, and k. The experimental conditions are found in Table A1 (SM) for the experiments from Figure 4. The volumes of the water and lube oil in the emulsion were calculated by scaling the weighted values with the densities (940 kg m^{-3} for lube oil [18,19] and 1000 kg m^{-3} for demineralized water at room temperature, because the two substances were weighted at room temperature).

It is unknown whether the SO_2(g) is absorbed into the water droplets, which are emulsified in the lube oil, the lube oil itself, or a mixture thereof. For the present purpose, Henry's constant for SO_2 in both water and lube oil were estimated. The temperature dependent Henry's constant for SO_2 in water was estimated from NIST [58]. Henry's constant for SO_2 in a fully formulated lube oil is more challenging

to assess since SO_2 reacts with the $CaCO_3$ in the lube oil; this makes the determination of only solubility in the lube oil difficult. Costa and Underhill [56], who studied uptake of SO_2 in different lube oil formulations at 25 ºC, also observed that SO_2 reacted with the base content in the lube oil, resulting in an overestimation of the 'solubility'. For the present study, Henry's constant at 25 ºC was calculated from the study of Costa and Underhill [56], based on a lube oil not containing base additives reacting with the SO_2. The resulting Henry's constant indicates that SO_2 is more soluble in water than in lube oil. A combined Henry's constant is derived based on the amount of water present initially in a lube oil sample in the following way, using a scaled resistance-like expression:

$$H_L = \frac{1}{\frac{1}{H_{oil}}\left(\frac{V_{oil}}{V_L}\right) + \frac{1}{H_{water}}\left(\frac{V_{water}}{V_L}\right)} \tag{16}$$

Here, H_{oil} and H_{water} are Henry's constants for lube oil and water, respectively, and V_{oil}, V_{water}, and V_L are the volumes of lube oil, water, and lube oil emulsion ($V_L = V_{oil} + V_{water}$). A detailed assessment of the derivation of the Henry's constants can be found in Supplementary Material.

The collected parameter $K_G a$ is then estimated. The specific gas-liquid interfacial area, a, is estimated as:

$$a = \frac{A_L}{V_L} = \frac{\pi R_{reactor}^2}{V_L} \tag{17}$$

where A_L represents the surface area between the gas phase and the liquid phase where the mass transfer takes place. For stagnant lube oil volume, A_L can be estimated from the radius of the batch reactor (3.15 cm). Evaluation of the resistance of the mass transfer of SO_2 from the gas phase to the liquid phase (see SM) indicated that mass transfer is controlled by the liquid-side resistance, viz, $K_G = k_L/H_L$. The liquid film mass transfer coefficient, k_L, is crudely estimated as [59],

$$k_L = \frac{D_L}{\delta_L} \tag{18}$$

where D_L is the diffusion coefficient of SO_2 in the liquid phase and δ_L is the liquid film thickness (see SM).

The only unknown in the model is thereby k, which is fitted to match the modeling results to the experimental data (conversion of $CaCO_3$ at specific τ, Figure 4). However, the estimated K_G and a, based on Eqs. (17) and (18), are based on a stagnant lube oil film and pure surface diffusion, which is far from the situation occurring in the stirred batch reactor, thus a correction factor is required. Therefore, $K_G a$ for the present system was estimated by use of the work from Meille et al. [60], who measured $k_L a$ ($K_G a = k_L a / H_L$) values as a function of stirrer speeds for different batch reactor dimension, finding that stirring of a liquid in a batch reactor contributed to an increased value of $k_L a$. Based on their work, a factor of 120 between $k_L a$ for a stagnant case (based on Eqs. (17) and (18) and the experimental parameters from Meille et al.) and an agitated case (stirrer speed of 600 rpm which was the stirrer speed applied in this work) was found and used in the subsequent modeling. The justifications and calculations are found in Supplementary Material.

3.2.7 Arrhenius plot

Based on the fitting of k at specific temperatures in the range 107-163 ºC, Arrhenius parameters were estimated (Eq. (19)), and the corresponding Arrhenius plot is shown in Figure 8.

$$\ln(k) = \ln(A) - \frac{E_a}{R}\frac{1}{T} \tag{19}$$

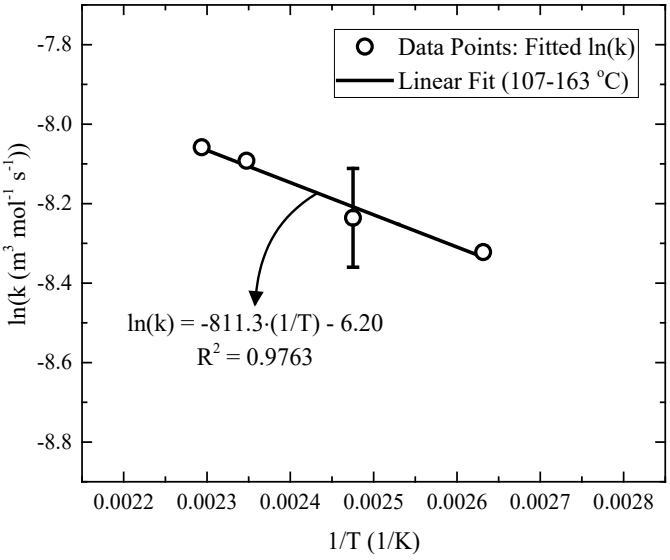

Figure 8. Arrhenius plot of the determined rate constant for $CaCO_3$ + SO_2 at temperatures in the range from 107 to 163 ºC. The linear fit, corresponding equation, and R^2 value are also shown. The error bars represent lower and upper $\ln(k)$ values determined from two similar experiments and the data point is the averaged value. From the trendline, the activation energy is determined to 6.7 kJ mol^{-1} and the pre-exponential factor to $2.03 \cdot 10^{-3}$ m^3 mol^{-1} s^{-1}.

A satisfactory linear fit is observed between $\ln(k)$ and $1/T$ from which an activation energy (E_a) of 6.7 kJ mol^{-1} and a pre-exponential factor (A) of $2.03 \cdot 10^{-3}$ m^3 mol^{-1} s^{-1} are determined. The uncertainty of the determination of k is indicated by the error bar. The temperature dependence of the reaction rate constant is small, in accordance with literature [53]. It was found that the SO_2 from the gas phase is readily absorbed into the lube oil, illustrated by a steep increase in the concentration curve for the SO_2 in the lube oil emulsion (see Figure A9 in SM).

3.2.8 Comparison between model and experimental data for varying residence time

Modeling predictions were compared with the experimental data from Figure 5, as shown in Figure 9. The model strongly overpredicts the conversion of $CaCO_3$ at longer residence times. It appears that the reaction becomes very slow and $CaSO_3$ reaches a plateau (see Figure A5 in SM). Instead, some

$CaCO_3$ is converted to $CaSO_4$ at a low rate, possibly because O_2 also has to participate in the reaction. Another explanation could be that the formed product, being $CaSO_3$ and/or $CaSO_4$, forms a product layer around the $CaCO_3$ reverse micelles acting as a diffusion barrier, thus significantly reducing the rate of reaction as shown in Figure 9.

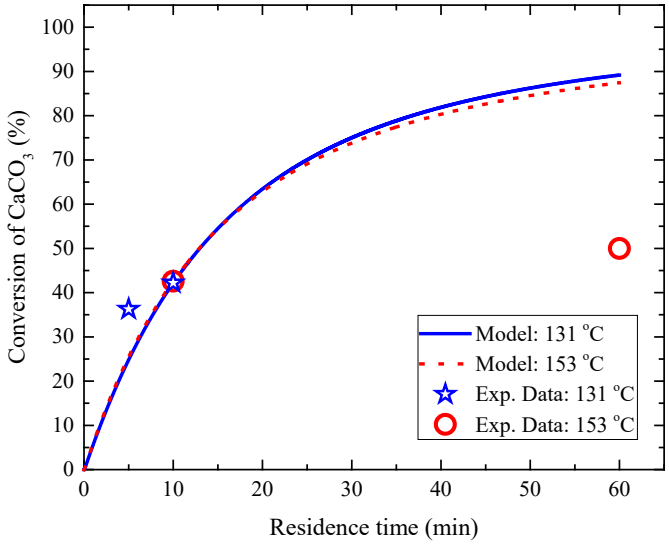

Figure 9. The effect of varying the residence time on the degree of conversion of $CaCO_3$ at temperatures of 131 and 153 ºC. The figure compares the model predictions with the experimental data from Figure 5.

3.2.9 Comparison between model and experimental data for varying initial water concentration

The effect of varying initial water concentration on the conversion of $CaCO_3$ is shown in Figure 10. The model captures the observed conversions within the uncertainty of the analysis technique. This means that the combined Henry's constant expression, Eq. (16), describes the water dependence sufficiently. The effect of water concentration is small; increasing the initial water concentration by a factor of 11 increases the conversion of $CaCO_3$ by only about 50%.

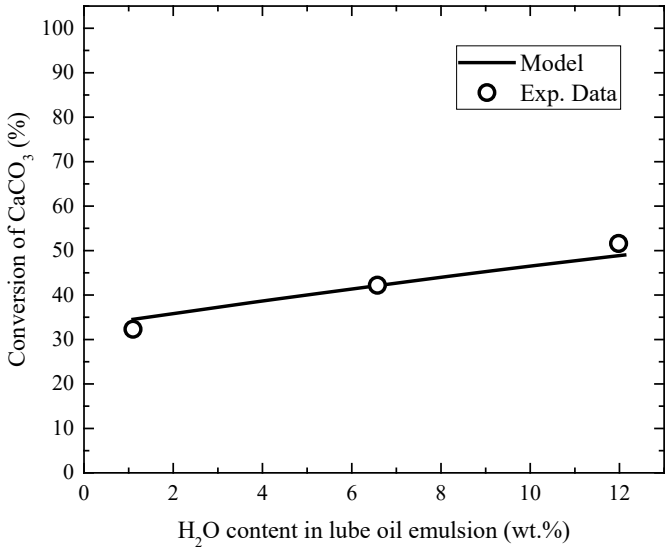

Figure 10. The effect of varying the initial water content in the lube oil emulsion on the degree of conversion of $CaCO_3$ at 131 ºC. The figure compares the model predictions with the experimental data from Figure 6.

3.2.10 Discussion of model simulations

The current results emphasize that accurate estimation of the correlated parameters $K_G a$ and k are required to predict the conversion of $CaCO_3$ by reaction with SO_2 precisely. Therefore, $K_G a$ was estimated by use of data from the literature [60], and Figure 8 was constructed. Whether these two parameters are estimated correctly is uncertain. The estimated values of $K_G a$ and k are one pair of parameters to the model that leads to simulated conversions of $CaCO_3$ in accordance with the experiments. However, an independent determination of the parameter $K_G a$, as done in the work of Meille et al. [60], is desirable. The effects of $K_G a$ and k on the conversion of $CaCO_3$ are simulated in Figure 11 for the experimental conditions of the 131 ºC experiment.

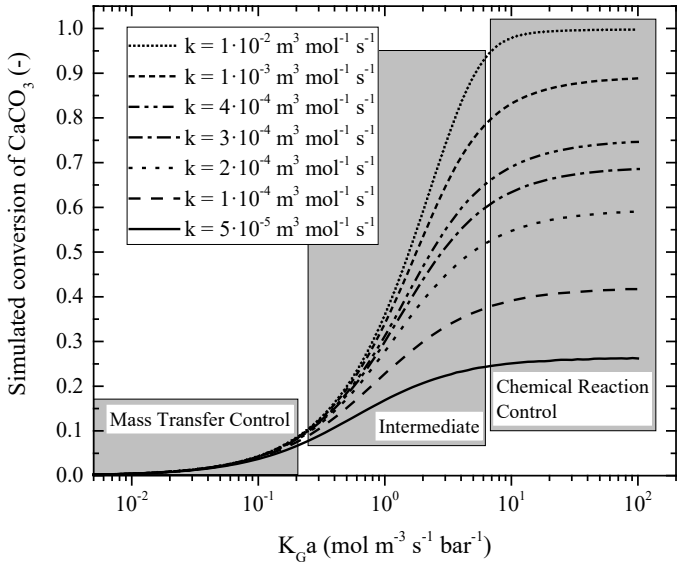

Figure 11. Simulated conversion of $CaCO_3$ as a function of $K_G a$ for seven different reaction rate constant values. The following parameters were used for the simulations: T=131 °C, τ=10 min, P_{total}=90 bar, $C^G_{SO_2,0}$=17.26 mol m^{-3}, 6.6 wt.% water in lube oil, and Ca/S = 0.96.

Three different regions are illustrated in Figure 11. At low $K_G a$ values, the reaction between SO_2 and $CaCO_3$ is mass transfer controlled, i.e., no effect of reaction rate is found. However, the mass transfer of SO_2 from the gas phase to the liquid phase is too low to achieve an observable degree of conversion of $CaCO_3$ (for the residence time of 10 min), or at least a degree comparable to the experimental degree of conversion. At high $K_G a$ values, only a minor effect of increasing $K_G a$ even further is found, while the effect of increasing k is significant. In-between, an intermediate region is found. At stagnant conditions, $K_G a$ was estimated to $1.6 \cdot 10^{-2}$ mol m^{-3} s^{-1} bar^{-1}, resulting in insignificant reaction of $CaCO_3$ (Figure 11). Accounting for stirring, $K_G a$ is strongly increased to 1.95 mol m^{-3} s^{-1} bar^{-1}; a value in the intermediate region of Figure 11 where both mass transfer and reaction control. Knowing the conversion of $CaCO_3$ (e.g., 42% at 131 °C) and $K_G a$, k was calculated to $2.65 \cdot 10^{-4}$ m^3 mol^{-1} s^{-1}, in accordance with Figure 11. In the intermediate region, a large change in k only lead to a minor effect on the conversion of $CaCO_3$. Because analysis uncertainties may be in the order of ±2 BN, this

has a large effect on the uncertainty of k as shown in Figure 8. The temperature dependency on k increases with $K_G a$. Increasing $K_G a$ a factor of five, the activation energy for the reaction becomes 23.5 kJ mol^{-1}.

In the model, only an overall reaction between SO_2 and $CaCO_3$ was considered. The mechanistic details of the reaction mechanism were thereby collected in the overall reaction rate constant, k. In reality, SO_2 may further react to HSO_3^- or SO_3^{2-} after entering the water in the lube oil emulsion. These reactions were not taken into account in the modeling and further studies are required to identify the exact reaction mechanism between SO_2, water, lube oil, and $CaCO_3$ reverse micelles.

3.3 Application of the batch reactor model to conditions in a large two-stroke diesel engine

The absorption and reaction rate expressions for the SO_2-$CaCO_3$ reaction derived from the modeling of the batch reactor experiments can be useful for computational fluid dynamics simulations of the effect of SO_2 on the consumption of $CaCO_3$ and accumulation of SO_2 in the lube oil at the cylinder liner in a large two-stroke marine diesel engine. Nevertheless, the batch reactor model offers a useful approximation to local conditions prevailing in a marine diesel engine and can be used to assess the importance of the SO_2-$CaCO_3$ reaction.

The entire combustion chamber in an engine can be considered as one batch reactor, where the gas volume is much larger than the lube oil volume, as in the case of the batch reactor experiments. However, the size of the combustion chamber changes as a stroke progresses. Assuming stagnation at different piston positions, each volume can therefore be considered as a batch reactor with associated partial pressure of SO_2 in the gas phase and lube oil emulsion volume. Under this circumstance, the batch reactor model of this work can assist in determining the absorption of SO_2 and subsequent degree of reaction between SO_2 and $CaCO_3$.

Assuming that all fuel-S is oxidized instantaneously to SO_2 prior to the expansion stroke, the SO_2 pressure will be highest when the piston is positioned in the very top of the cylinder (at top dead

center, TDC). As the expansion stroke progresses, the partial pressure of SO_2 in the gas phase decreases as the combustion chamber volume increases, the combustion gas is exhausted, and later further diluted by the intake air. Ideally, this leads to desorption of SO_2 from the lube oil emulsion due to the changed SO_2 concentration gradient across the gas-liquid interface. However, due to the fast passage of the piston, the desorption rate of SO_2 is presumably too slow to actually come into force. This is supported by observations from the batch reactor experiments. The absorption rate of SO_2 decreases as the expansion stroke progresses and is negligible during the compression stroke where the cylinder gas products have been ventilated and replaced by fresh intake air. At a local, discretized volume section of the cylinder liner, the partial pressure of SO_2 is thus constantly changing.

To keep it simple in the modeling, the partial pressure of SO_2 in the gas phase is assumed to be constant for each piston position and the residence time for the simulations is chosen as that of the lube oil in the engine. Assuming that the partial pressure of SO_2 is constant throughout the residence time is a worst case scenario and may ultimately lead to an overestimation of the degree of conversion of $CaCO_3$ from SO_2. Average lube oil residence times of up to 4 min in an engine have been estimated [1,18,61].

3.3.1 Engine simulation: the SO_2-$CaCO_3$ reaction

The $CaCO_3$ consumption from SO_2 was modeled at worst-case engine conditions, i.e., conditions that increase the $CaCO_3$ conversion (see SM). The simulations revealed that the $CaCO_3$ consumption is highest near TDC (up to 40% conversion), due to the high SO_2 concentration here. However, the consumption of $CaCO_3$ steeply decreases further down the vertical direction of the cylinder liner. When sampling a lube oil off-shore, it is an averaged $CaCO_3$ conversion throughout the whole vertical direction of the cylinder liner that is sampled. Simulating the average $CaCO_3$ conversion throughout the vertical direction of the cylinder gave a value of 7.9%. A typical recommendation is to achieve

between 50-75% conversion of $CaCO_3$ in practice [4], so SO_2 is only responsible for a minor part of the consumption of $CaCO_3$ in practice. Furthermore, the input data to the model (presented in Table A5 in SM) are chosen in order to enhance the conversion of $CaCO_3$, e.g., the chosen temperature, load, sulfur content in the fuel, residence time, etc. That means, under a worst-case scenario, maximum 7.9% of the available $CaCO_3$ in lube oil can be neutralized by reaction with SO_2. A more detailed description of these simulations can be found elsewhere [35] or in Supplementary Material.

3.3.2 Engine simulation: Competition between SO_2-$CaCO_3$ and H_2SO_4-$CaCO_3$ reactions

The previous section showed that around 40% of the $CaCO_3$ could potentially be consumed by SO_2 in the lube oil at worst-case conditions near TDC (Figure A11 in SM, for a residence time of 10 min). However, if H_2SO_4 is present in the lube oil emulsion, the effect of SO_2 on the consumption of $CaCO_3$ may be even smaller. The H_2SO_4-$CaCO_3$ reaction has previously been investigated by the authors [19]. Their simulations indicated that 38% of the $CaCO_3$ is consumed after a residence time of 0.5 s, for a temperature of 100 ^oC and for a Ca/S molar ratio equal to 1 (remaining parameters: radius of H_2SO_4 droplets: 0.5 μm, 100 BN lube oil, and concentration of H_2SO_4 droplets: $18 \cdot 10^3$ mol m^{-3}). Comparing this conversion degree to the one determined in this work reveals that the rate of the H_2SO_4-$CaCO_3$ reaction is much larger than the SO_2-$CaCO_3$ reaction. Thus, if both SO_2 and H_2SO_4 are present in the lube oil film, the $CaCO_3$ would preferentially react with H_2SO_4. If H_2SO_4 is limited compared to $CaCO_3$, on a molar basis, then $CaCO_3$ would first consume the majority of the H_2SO_4, followed by reaction with SO_2. However, H_2SO_4 gradually condenses onto the cylinder liner (during each expansion stroke), which means that H_2SO_4 may be available for reaction with $CaCO_3$ continually. Thus it appears that the significance of SO_2 for consumption of $CaCO_3$ reverse micelles is negligible in a marine diesel engine application. Moreover, the batch reactor experiments revealed that $CaSO_3$ was the main product from the SO_2-$CaCO_3$ reaction, hence maintaining the neutralization

ability of the lube oil towards H_2SO_4. This suggests that the actual $CaCO_3$ consumption from SO_2 may be significantly smaller in an engine application than the simulations estimate.

It is also possible to make a direct comparison of the H_2SO_4-$CaCO_3$ and SO_2-$CaCO_3$ reactions under conditions relevant for the engine application, using the batch reactor model with an extended reaction mechanism (see SM). However, the competition between the two reactions depends strongly on the initial concentration of H_2SO_4 in the lube oil emulsion. It was found that the H_2SO_4-$CaCO_3$ reaction generally dominates over the SO_2-$CaCO_3$ reaction. The dominance increases for increasing temperature, decreasing SO_2 partial pressure, and increasing initial H_2SO_4 concentration. Near TDC, the temperature is highest and most H_2SO_4 is condensing [1,4,15,16], and toward the bottom of the cylinder liner, the partial pressure of SO_2 in the gas phase is rapidly declining. This supports the finding that H_2SO_4 is responsible for consuming the vast majority of the $CaCO_3$ in the lube oil in an engine application.

Nagaki and Korematsu [48] report that increased absorption of SO_2 in the lube oil film by EGR (Exhaust Gas Recirculation) increases the wear. However, the consumption of base additives remained unchanged, contradicting their suggestion that H_2SO_4 is formed from SO_2 in the lube oil film [46–48]. Presumably, SO_2 is not being responsible for consuming $CaCO_3$, but may, in combination with water, have a corrosive effect on the cylinder liner surface. As shown in this study, SO_2 is absorbed into the lube oil film and interaction with the liner is thereby possible. If local conditions allow a large amount of water to condense [15], SO_2(aq) may have direct access to the liner material, possibly promoting corrosive wear.

4 Conclusions

The reaction between gaseous SO_2 and $CaCO_3$ reverse micelles in lube oil has been studied using a batch reactor setup, and a mathematical model was set up in order to extract kinetic parameters of the

reaction. The model was then used to predict the significance of the SO_2-$CaCO_3$ reaction at worst-case conditions similar to the ones prevailing in a large two-stroke marine diesel engine.

The experimental work in a batch reactor revealed that SO_2 and $CaCO_3$ do react in lube oil, initially forming $CaSO_3$, but at increased residence times and temperatures, also $CaSO_4$. Presence of water promoted the conversion of $CaCO_3$, presumably due to an increased absorption rate of SO_2 in the lube oil emulsion. The effect of temperature on the reaction rate was minor because the absorption of SO_2 decreases at increased temperature. Modeling of the experimental data showed that the mass transfer coefficient, K_G, and reaction rate constant, k, are highly correlated and multiple solutions can be found when fitting the model to the experimental data. Therefore, K_G was estimated by use of experiments from literature [60], and a resulting Arrhenius plot was constructed from which kinetic parameters were determined.

The batch reactor model was then used to predict the $CaCO_3$ conversion by reaction with SO_2 at worst-case conditions similar to the ones prevailing in a large diesel engine by discretizing the vertical direction of the cylinder liner. The simulations revealed that the $CaCO_3$ conversion highly depended on the SO_2 concentration in the gas phase and the highest conversion of $CaCO_3$ was therefore at TDC. However, the SO_2 concentration in the gas phase readily decreases as the expansion stroke progresses and the averaged worst-case $CaCO_3$ conversion determined (7.9%) cannot explain the $CaCO_3$ conversions found in practice. The present study also showed that, when H_2SO_4 is present in the lube oil film, it will be converting the major part of the $CaCO_3$. It is concluded that the reaction SO_2-$CaCO_3$ is not important for consumption of $CaCO_3$ reverse micelles in the lube oil in a two-stroke marine diesel engine. Whether SO_2(aq) can react with the cylinder liner material and contribute to corrosion is, however, unknown. The results of this study, together with the earlier work on the H_2SO_4-$CaCO_3$ [19], are expected to facilitate and support further studies on how to control corrosive wear in large two-stroke marine diesel engines at a minimal lube oil consumption.

Declaration of interest

The authors declare that they have no conflict of interest.

Acknowledgments

This work is part of the Combustion and Harmful Emission Control (CHEC) research center at the Department of Chemical and Biochemical Engineering at the Technical University of Denmark. The project is funded by the Innovation Fund Denmark and cosponsored by MAN Energy Solutions and the Technical University of Denmark through the SULCOR project under grant 4106-00028B.

Appendix A. Supplementary Material

Supplementary data to this article can be found online at .

Nomenclature

a = Specific gas-liquid interfacial area [m^2 m^{-3}]

A = Pre-exponential factor [m^3 mol^{-1} s^{-1}]

A_L = Stagnant area of lube oil emulsion [m^2]

BN = Base number [(mg KOH) $(g\ oil)^{-1}$]

Ca/S = Initial molar ratio of $CaCO_3$ in lube oil to SO_2 in gas phase [mol mol^{-1}]

C_i^j = Concentration of component i in component j [mol m^{-3}]

D = Diameter of the cylinder [m]

D_i = Diffusion coefficient of SO_2 in component i [m^2 s^{-1}]

E_a = Activation energy [J mol^{-1}]

f = Last subvolume number [-]

h = Height of a subvolume [m]

H = Height of cylinder liner [m]

H_i = Henry's constant of SO_2 in component i [bar m^3 mol^{-1}]

i = Component i [-]

j = Component j [-]

k = Reaction rate constant [m^3 mol^{-1} s^{-1}]

k_G = Gas film mass transfer coefficient [mol m^{-2} s^{-1} bar^{-1}]

K_G = Overall gas-side mass transfer coefficient of SO_2 [mol m^{-2} bar^{-1} s^{-1}]

k_L = Liquid film mass transfer coefficient [m s^{-1}]

l = Subvolume numer [-]

N_i = Absorption rate of component i from the gas phase to the lube oil emulsion [mol m^{-3} s^{-1}]

p_i^j = Bulk partial pressure of component i in component j [bar]

P = Pressure in batch reactor [bar]

R = Ideal gas constant, 8.314 [J mol^{-1} K^{-1}]

$(-r_A)$ = Reaction rate [mol m^{-3} s^{-1}]

$R_{reactor}$ = Radius of batch reactor [m]

t = Time [s]

T = Temperature [^oC or K]

V_i = Volume of component i [m^3]

Greek Letters

δ_L = Liquid film thickness [m]

τ = Residence time [s]

Superscripts and subscripts

G = Gas phase

L = Lube oil emulsion (lube oil + water)

oil = Lube oil

References

[1] L. García, S. Gehle, J. Schakel, Impact of Low Load Operation in Modern Low Speed 2-Stroke Diesel Engines on Cylinder Liner Wear Caused by Increased Acid Condensation, J. JIME. 49 (2014) 100–106.

[2] MAN Diesel & Turbo, Service Letter SL2014-587/JAP, (2014).

[3] A. Adamkiewicz, J. Drzewieniecki, Operational Evaluation of Piston Ring Wear in Large Marine Diesel Engines, J. Polish CIMAC. (2012). http://www.polishcimac.pl/Papers1/2012/001.pdf.

[4] CIMAC Working Group 8 "Marine Lubricants," CIMAC Guideline Cold Corrosion in Marine Two Stroke Engines, (2017).

[5] C.H. Bovington, Friction, Wear and the Role of Additives in Controlling Them, in: R.M. Mortier, M.F. Fox, S.T. Orszulik (Eds.), Chem. Technol. Lubr., Springer Netherlands, Dordrecht, 2010: pp. 77–105. doi:10.1023/b105569_3.

[6] D. Atkinson, Onboard condition monitoring of cold corrosion in two-stroke marine diesel engines, 11th Int. Conf. Cond. Monit. Mach. Fail. Prev. Technol. C. 2014 / MFPT 2014. 5 (2014) 17–22. http://www.scopus.com/inward/record.url?eid=2-s2.0-84918578542&partnerID=tZOtx3y1.

[7] I. Marković, R.H. Ottewill, D.J. Cebula, I. Field, J.F. Marsh, Small angle neutron scattering studies on non-aqueous dispersions of calcium carbonate - Part I. The Guinier approach, Colloid Polym. Sci. 262 (1984) 648–656. doi:10.1007/BF01452457.

[8] International Maritime Organization (IMO), Sulphur oxides (SOx) and Particulate Matter (PM) – Regulation 14, (n.d.). http://www.imo.org/en/OurWork/Environment/PollutionPrevention/AirPollution/Pages/Sulphur-oxides-(SOx)-%E2%80%93-Regulation-14.aspx (accessed October 22, 2018).

[9] D.M.S. Jacobsen, J.M. Pedersen, J. Svensson, S. Mayer, Cylinder Lube Oil Experiences and New Development for the MAN B&W Two-stroke Engines, in: 28th CIMAC World Congr., Helsinki, 2016.

[10] R. Cordtz, The Influence of Fuel Sulfur on the Operation of Large Two-Stroke Marine Diesel Engines. Ph.D. Dissertation, Technical University of Denmark, Kgs. Lyngby, 2015.

[11] O. Christensen, Cylinder lubrication of two-stroke crosshead marine diesel engines, Wärtsilä Tech. J. (2010) 39–48.

[12] K.M. Pang, N. Karvounis, J.H. Walther, J. Schramm, P. Glarborg, S. Mayer, Modelling of temporal and spatial evolution of sulphur oxides and sulphuric acid under large, two-stroke marine engine-like conditions using integrated CFD-chemical kinetics, Appl. Energy. 193 (2017) 60–73. doi:10.1016/j.apenergy.2017.02.020.

[13] R.L. Cordtz, J. Schramm, R. Rabe, Investigating SO_3 Formation from the Combustion of Heavy Fuel Oil in a Four-Stroke Medium Speed Test Engine, Energy Fuels. 27 (2013) 6279–6286. doi:10.1021/ef4014696.

[14] R. Cordtz, J. Schramm, A. Andreasen, S.S. Eskildsen, S. Mayer, Modeling the distribution of sulfur compounds in a large two stroke diesel engine, Energy Fuels. 27 (2013) 1652–1660. doi:10.1021/ef301793a.

[15] R. Cordtz, S. Mayer, S.S. Eskildsen, J. Schramm, Modeling the condensation of sulfuric acid and water on the cylinder liner of a large two-stroke marine diesel engine, J. Mar. Sci. Technol. 23 (2018) 178–187. doi:10.1007/s00773-017-0455-9.

[16] N. Karvounis, K.M. Pang, S. Mayer, J.H. Walther, Numerical simulation of condensation of sulfuric acid and water in a large two-stroke marine diesel engine, Appl. Energy. 211 (2018) 1009–1020. doi:10.1016/j.apenergy.2017.11.085.

[17] J. Schramm, S. Henningsen, S.C. Sorenson, Modelling of Corrosion of Cylinder Liner in

Diesel Engines Caused by Sulphur in the Diesel Fuel, in: SAE Tech. Pap., SAE International, 1994: pp. 1–10. doi:10.4271/940818.

[18] K.H. Lejre, S. Kiil, P. Glarborg, H. Christensen, S. Mayer, Reaction of Sulfuric Acid in Lube Oil: Implications for Large Two-Stroke Diesel Engines, in: Proc. ASME 2017 Intern. Combust. Engine Div. Fall Tech. Conf., ASME, Seattle, United States, 2017: pp. 1–10. doi:10.1115/ICEF2017-3580.

[19] K.H. Lejre, P. Glarborg, H. Christensen, S. Mayer, S. Kiil, Mixed Flow Reactor Experiments and Modeling of Sulfuric Acid Neutralization in Lube Oil for Large Two-Stroke Diesel Engines, Ind. Eng. Chem. Res. 58 (2019) 138–155. doi:10.1021/acs.iecr.8b05808.

[20] R.C. Wu, K.D. Papadopoulos, C.B. Campbell, Visualization Test for Neutralization of Acids by Marine Cylinder Lubricants, AIChE J. 45 (1999) 2011–2017. doi:10.1002/aic.690450917.

[21] R.C. Wu, K.D. Papadopoulos, C.B. Campbell, Acid-neutralizing of marine cylinder lubricants: Measurements and effects of dispersants, AIChE J. 46 (2000) 1471–1477. doi:10.1002/aic.690460720.

[22] R.C. Wu, C.B. Campbell, K.D. Papadopoulos, Acid-Neutralizing of Marine Cylinder Lubricants: Effects of Nonionic Surfactants, Ind. Eng. Chem. Res. 39 (2000) 3926–3931. doi:10.1021/ie000039c.

[23] J. Fu, Y. Lu, C.B. Campbell, K.D. Papadopoulos, Temperature and acid droplet size effects in acid neutralization of marine cylinder lubricants, Tribol. Lett. 22 (2006) 221–225. doi:10.1007/s11249-006-9082-z.

[24] J. Fu, Y. Lu, C.B. Campbell, K.D. Papadopoulos, Acid Neutralization by Marine Cylinder Lubricants Inside a Heating Capillary: Strong/Weak-Stick Collision Mechanisms, Ind. Eng. Chem. Res. 45 (2006) 5619–5627. doi:10.1021/ie051209u.

[25] J. Fu, K.D. Papadopoulos, Y. Lu, C.B. Campbell, Ostwald ripening: A decisive cause of

cylinder corrosive wear, Tribol. Lett. 27 (2007) 21–24. doi:10.1007/s11249-007-9198-9.

[26] M. Garcia-Bermudes, R. Rausa, K. Papadopoulos, Vertically-oriented-capillary video-microscopy: Drops levitated by a (Reacting) fluid, Ind. Eng. Chem. Res. 50 (2011) 14142–14147. doi:10.1021/ie201409e.

[27] M. Garcia-Bermudes, R. Rausa, K. Papadopoulos, Formation of Colloidal Shells on Acidic Droplets Undergoing Neutralization in Marine Diesel Engine Cylinder Oils, Tribol. Lett. 51 (2013) 85–92. doi:10.1007/s11249-013-0149-3.

[28] Y. Duan, R. Rausa, Q. Zhao, K.D. Papadopoulos, Neutralization Mechanism of Acetic Acid by Overbased Colloidal Nanoparticles, Tribol. Lett. 64 (2016) 1–11. doi:10.1007/s11249-016-0742-3.

[29] D.C. Hone, B.H. Robinson, D.C. Steytler, R.W. Glyde, J.A. Cleverley, Acid-base chemistry in high-performance lubricating oils, Can. J. Chem. 77 (1999) 842–848.

[30] D.C. Hone, B.H. Robinson, D.C. Steytler, R.W. Glyde, J.R. Galsworthy, Mechanism of Acid Neutralization by Overbased Colloidal Additives in Hydrocarbon Media, Langmuir. 16 (2000) 340–346. doi:10.1021/la9904354.

[31] D. Hone, B. Robinson, J. Galsworthy, R. Glyde, Colloidal Chemistry of Lubricating Oils, in: J. Texter (Ed.), React. Synth. Surfactant Syst., CRC Press, 2001: pp. 385–394. doi:10.1201/9780203908662.

[32] K. Hosonuma, K. Tamura, Acid Neutralization of Overbased Detergents (Part 1) Neutralization in the Test Methods of ASTM Base Number, J. Japan Pet. Inst. 27 (1984) 101–107. doi:10.1627/jpi1958.27.101.

[33] K. Hosonuma, K. Tamura, Acid Neutralization of Overbased Detergents (Part 2) Neutralization with Sulfuric Acid Emulsion, J. Japan Pet. Inst. 27 (1984) 108–113. doi:10.1627/jpi1958.27.108.

[34] J.-P. Roman, New method of measurement in thin film of the neutralization of marine lubricants for low-speed and medium-speed diesel engines, in: CIMAC Congr. 1998, Copenhagen, Copenhagen, 1998: pp. 913–926.

[35] K.H. Lejre, Mechanisms of sulfur dioxide and sulfuric acid neutralization in lube oil for marine diesel engines. Ph.D. Dissertation, Technical University of Denmark, Kgs. Lyngby, 2019.

[36] K. Akiyama, K. Masunaga, K. Kado, T. Yoshioka, Cylinder Wear Mechanism in an EGR-Equipped Diesel Engine and Wear Protection by the Engine Oil. Paper 872158, SAE Int. (1987) 1–7.

[37] C. Amblard, New Chemistry to Protect against Cold Corrosion in Marine Cylinder Lubricants, J. Japan Inst. Mar. Eng. 50 (2015) 54–62. doi:10.5988/jime.50.759.

[38] A.M. Buck, A.G. Cattaneo, R.A. Coit, J.A. Edgar, A.R. Isitt, Engine Lubricating Oils for the Reduction of Wear, in: 3rd World Pet. Congr. 28 May-6 June, Hague, Netherlands, 1951: pp. 405–412.

[39] A.G. Macdonald, F.H. Stott, The Corrosive Wear of Cast Iron in Oil-Sulphuric Acid Mixtures, Corros. Sci. 28 (1988) 485–501.

[40] D.W. Golothan, Review of the Causes of Cylinder Wear in Marine Diesel Engines, Inst. Mar. Eng. Trans. 90 (1978) 137–163.

[41] G. McConnell, W.S. Nathan, A wear theory for low speed diesel engines burning residual fuel, Wear. 5 (1962) 43–54. doi:10.1016/0043-1648(62)90179-5.

[42] F.H. Stott, A.G. Macdonald, The influence of acid strength on the corrosive wear of grey cast irons in oil-sulphuric acid mixtures, Wear. 122 (1988) 343–361. doi:10.1016/0043-1648(88)90019-1.

[43] A.K. van Helden, M.C. Valentijn, H.M.J. van Doornt, Corrosive wear in crosshead diesel engines, Tribol. Int. 22 (1989) 189–193. doi:10.1016/0301-679X(89)90156-4.

[44] Y. Yahagi, Corrosive Wear of Diesel Engine Cylinder Bore, Tribol. Int. 20 (1987) 365–373. doi:10.1016/0301-679X(87)90065-X.

[45] J.A. McGeehan, A. V. Kulkarni, Mechanism of Wear Control by the Lubricant in Diesel Engines, No. 872029, in: SAE Tech. Pap. Ser., 1987: pp. 1–14. doi:10.4271/872029.

[46] H. Nagaki, K. Korematsu, Relation Between Diffusion Process of Sulfur Oxides in Exhaust Gas into Oil Film and Wear of Cylinder Liner and Piston Rings in Diesel Engines, SAE Pap. (1991). doi:10.4271/912400.

[47] H. Nagaki, K. Korematsu, Effect of Sulfur Dioxide in Recirculated Exhaust Gas on Wear within Diesel Engines - (Relationship between Wear and Amount of SO_2 Absorbed by Lubricating Oil Film), JSME Int. J. Ser. B-Fluids Therm. Eng. 38 (1995) 465–474.

[48] H. Nagaki, K. Korematsu, Effect of SO_2 in Recirculated Exhaust Gas on Wear in Diesel Engine - (Effect of SO_2 Added to Intake Air on Wear), JSME Int. J. Ser. B-Fluids Therm. Eng. 39 (1996) 193–201.

[49] D.W. Naegeli, H.W. Marbach, Role of Sulfur Oxides in Wear and Deposit Formation in Army Diesel Engines. Interim Report BFLRF No. 248, Contract No. DAAK70-87-C-0043, (1988).

[50] S. Kiil, Experimental and Theoretical Investigations of Wet Flue Gas Desulphurisation. Ph.D. Dissertation, Technical University of Denmark, Kgs. Lyngby, 1998.

[51] P. Córdoba, Status of Flue Gas Desulphurisation (FGD) systems from coal-fired power plants: Overview of the physic-chemical control processes of wet limestone FGDs, Fuel. 144 (2015) 274–286. doi:10.1016/j.fuel.2014.12.065.

[52] S. Kiil, M.L. Michelsen, K. Dam-Johansen, Experimental Investigation and Modeling of a Wet Flue Gas Desulfurization Pilot Plant, Ind. Eng. Chem. Res. 37 (1998) 2792–2806. doi:10.1021/ie9709446.

[53] J. Klingspor, H.T. Karlsson, I. Bjerle, A Kinetic Study of the Dry SO_2-Limestone Reaction at

Low Temperature, Chem. Eng. Commun. 22 (1983) 81–103. doi:10.1080/00986448308940047.

[54] J. Baltrusaitis, C.R. Usher, V.H. Grassian, Reactions of sulfur dioxide on calcium carbonate single crystal and particle surfaces at the adsorbed water carbonate interface, Phys. Chem. Chem. Phys. 9 (2007) 3011–3024. doi:10.1039/b617697f.

[55] H.A. Al-Hosney, V.H. Grassian, Water, sulfur dioxide and nitric acid adsorption on calcium carbonate: A transmission and ATR-FTIR study, Phys. Chem. Chem. Phys. 7 (2005) 1266. doi:10.1039/b417872f.

[56] D.L. Costa, D. Underhill, Solubility and reactivity of sulfur dioxide in various oils, Am. Ind. Hyg. Assoc. J. 37 (1976) 46–51. doi:10.1080/0002889768507406.

[57] ASTM International, ASTM 2896-11. Standard Test Method for Base Number of Petroleum Products by Potentiometric Perchloric Acid Titration, (2011). doi:10.1520/D7751-16.

[58] NIST Chemistry WebBook:, (n.d.). https://webbook.nist.gov/chemistry.

[59] P.G. Smith, Introduction to Food Process Engineering, Springer US, Boston, MA, 2011. doi:10.1007/978-1-4419-7662-8.

[60] V. Meille, N. Pestre, P. Fongarland, C. de Bellefon, Gas/Liquid Mass Transfer in Small Laboratory Batch Reactors: Comparison of Methods, Ind. Eng. Chem. Res. 43 (2004) 924–927. doi:10.1021/ie030569j.

[61] J. Hammett, Utilising the Latest Findings Engine Oil Stress from Field & Laboratory Engine Testing, J. JIME. 49 (2014) 6–13.